Computations of dendrites in 3-D and comparison with microgravity experiments

Y. B. Altundas and G. Caginalp
University of Pittsburgh
Pittsburgh, PA 15260
ybast@pitt.edu
caginalp@pitt.edu

Abstract. The phase field model is used to compute numerically the temporal evolution of the interface for solidification of a single needle crystal of succinonitrile (SCN) in a three dimensional cylindrical domain with conditions satisfying microgravity experiments. The numerical results for the tip velocity are (i) consistent with the experiments, (ii) compatible with the experimental conclusion that tip velocity does not increase for larger anisotropy (e.g. for pivalic acid), (iii) different for 3-D versus 2-D by a factor of approximately (D-1), (iv) strongly dependent on physical value of the kinetic coefficent in the model.

Keywords: solidification, phase field equations, dendrite, single needle crystal, succinonitrile, microgravity.

PACS numbers: 68.70.+w, 05.70.Ln, 64.70.Dv, 81.30Fb

The temporal evolution of an interface during solidification has been under intensive study by physicists and material scientists for several decades. The interface velocity and shape have important consequences for practical metallurgy, as well as the theory, e.g., velocity selection mechanism and nonlinear theory of interfaces. The simplest observed microstructure is the single needle crystal or dendrite, which has been modeled in an early study by Ivantsov [1] as a parabaloid growing at a constant velocity, v_0, with tip radius,

R, subject to the heat diffusion equation and latent heat considerations at the interface. With the interface stipulated to be at the melting temperature, the absence of an additional length scale implies the existence of an infinite spectrum of pairs of velocities and tip radii, (v_0, R_0). Experimentally it has been observed that a unique pair (v_{exp}, R_{exp}) is selected, so that the tip velocity is constant throughout the experiment, and is independent of initial conditions.

The theoretical mechanism for this velocity selection has been the focus of much of the theoretical research on the subject (see, for example [2-7]). The emergence of the capillarity length associated with the surface tension as an additional length scale has provided an explanation for the selection mechanism. Advances in computational power and a better understanding of interface models and their computation have opened up the possibility of comparing experimental values for the tip velocity with the numerical computations. This is nevertheless a difficult computational issue in part due to the large differences in length scales that range from 1 cm for the size of the experimental region, to 10^{-6} cm for the capillarity length, to 10^{-8} cm interface thickness length.

One perspective into the theoretical and numerical study of such interfaces has been provided by the phase field model introduced in [8,9] in which a phase, or order parameter, ϕ, and temperature, T, are coupled through a pair of partial differential equations described below. In physical terms, the width of the transition region exhibited by ϕ is Angstroms. In the 1980's two key results facilitated the use of these equations for computation of physically relevant phenomena. If the equations are properly scaled one can (i) identify each of the physical parameters, such as the surface tension, and attain the sharp interface

problem as a limit [10,11], and (ii) use the interface thickness, ϵ, as a free parameter, since the motion of the interface is independent of this parameter [12]. The latter result thereby opened the door to computations with realistic material parameters, by removing the issue of small interface thickness. However, the difference in scale between the capillarity length and overall dimensions still pose a computational challenge.

More recently, several computations, have been done using the phase field model [13-19], with some 3D computations in [14] and [15] utilizing the model of [22], that will be compared with our results below.

In this paper we present computations that have the following novel features:

(A) We perform numerical computations for a cylindrical region in three dimensional space by utilizing rotational symmetry. This allows us to compare the velocity and tip radius with the actual experiments in a meaningful way.

(B) The calculations utilize the parameters and boundary conditions of the IDGE microgravity experiments for succinonitrile (SCN) [20]. All previous experiments done under normal gravity conditions introduced convection. Hence this provides the first opportunity to compare experiments in the absence of convection to theory that also excludes convection. Our results for tip velocity compare favorably with the data of these experiments.

(C) The role of anisotropy in velocity selection has been noted in the computational references cited above. Nevertheless, Glicksman and Singh [21] compare experimental tip velocities of SCN with pivalic acid (PVA) whose coefficient of surface tension anisotropy (defined below) differ by a factor of 10 but are otherwise similar, except perhaps for the

kinetic coefficient. The graph of their data ([21] figure 7) indicates that the tip velocities of the two materials differ by less than 10 percent.

We perform two sets of calculations in which all parameters are identical (SCN values) except for the anisotropy coefficient. Our computations confirm the result that the velocities are nearly identical, which is somewhat paradoxical since one might conjecture that the role of anisotropy in selection might lead to a mechanism for adjusting velocity through the magnitude of anisotropy.

(D) Most of the previous numerical computations that simulate the interface growth were done in 2-D. Our computations shows that the 2-D and 3-D computations differ by a factor of approximately (D–1).

(E) The role of the kinetic coefficient [see definition of α below equation (2)] is subtle, and this material parameter is often set to zero, for convenience, in theoretical and computational studies. We find, however, that there is a significant difference in the tip velocity when all other parameters are held fixed while this coefficient is varied. This suggests that further experiments and theory on this subject may lead to a deeper understanding of dendritic phenomena.

In the computations below we use a version of the phase field equations introduced in [22], for which the phase or order parameter, $\phi(\vec{x}, t)$, as a function of spacial point, $\vec{x}$, and time, t, is exactly -1 in the solid and $+1$ in the liquid. We define the dimensionless temperature, u, and the capillarity length, d_0, by

$$u(x,t) = \frac{\mathrm{T} - \mathrm{T}_m}{l_v/c_v}, \qquad d_o = \frac{\sigma\ c_v}{[s]_E\ l_v}$$

where T_m, l_v and c_v are the melting temperature, latent heat and specific heat per unit volume of the material. Thus, we write the dimensionless phase field equations as following:

$$u_t + \tfrac{1}{2}\phi_t = D\nabla^2 u \tag{1}$$

$$\alpha\epsilon^2\phi_t = \epsilon^2\nabla^2\phi + g(\phi) + \tfrac{5}{8}\tfrac{\epsilon}{d_o}uf'(\phi) \tag{2}$$

where

$$g(\phi) = \tfrac{1}{2}(\phi - \phi^3), \qquad f'(\phi) = (1-\phi^2)^2, \qquad D = \frac{K}{C_v},$$

and the interface is defined by $\Gamma(x,t) = \{x \in \Omega : \phi(x,t) = 0\}$. In the limit as $\epsilon \mapsto 0$, the temperature at the interface satisfies the kinetic Gibbs-Thomson relation

$$u = -d_0\kappa - \alpha d_0\, v_n,$$

where v_n is the normal velocity and α is the kinetic coefficient [8,22].

In order to simulate the interfacial growth of a 3-D single needle dendrite for the compound succinonitrile (SCN) in a cylindrical geometry (under the assumption that the needle grows symmetrically), we consider a domain which is a cylindrical chamber filled with the pure melt. A small radially symmetric seed is placed at the bottom center of the chamber. We denote the flat surface of the cylinder where the seed is placed by S_1, the flat surface across from the seed (i.e. far field) by S_2, and the curved surface around the cylinder by S_3. Thus we define the boundary and initial conditions below as follows. The temperature at S_2 and S_3 are kept at the constant supercooling value

u_∞. The temperature at S_2 is also kept at a constant (in time) temperature, but declines exponentially from $u = 0$ on the interface of the seed to the intersection of S_2 with S_3, where $u = u_\infty$.

In particular, the boundary condition for u on S_2 is given as $u_{trav}(s, 0)$ where s is the distance from the seed interface, and

$$u_{trav}(z,t) = \begin{cases} u_\infty \left(1 - exp\{-v(z - vt/|u_\infty|)/(D|u_\infty|)\}\right) & z > vt/(u_\infty) \\ 0 & z \leq vt/(u_\infty) \end{cases} \tag{3}$$

is a plane wave solution to a 1-D problem. The order parameter is initially set to its equilibrum value

$$\phi(\rho) = tanh\left((\rho - vt)/(2\epsilon)\right) \tag{4}$$

where ρ is the signed distance (positive in the liquid) from the interface [22]. The boundary conditions for ϕ are defined to be compatible with those on the temperature.

The anisotropy is incorporated into the equations through the surface tension where one has precise and quantitative experimental data in order to utilize the experimentally observed quantities and parameters. Thus, we write the surface tension as

$$\sigma(\theta) = \sigma_0[1 - (\mathrm{M}^2 - 1)\delta_\sigma \cos(\mathrm{M}(\theta - \theta_0)] \tag{5}$$

where θ is the angle between the horizontal direction and the normal of the solid-liquid interface. Here, θ_0 is preferred growth direction, and σ_0 is an experimental constant for the

particular material, as is $(\mathrm{M}^2-1)\delta_\sigma$. Hence, if $(\mathrm{M}^2-1)\delta_\sigma < 1$ is satisfied then the curvature has its maximum at $\theta = \theta_0$ [12]. This is consistent with the experimental evidence [21].

For the computational convenience, we take a vertical cross section through the origin. Upon writing the equations (1) and (2) in cylindrical coordinates, the terms involving θ drops and we get a simplified form of the phase field equations in a cylindrical coordinate system.

The discretization of the equations is done implicitly in space and explicitly in time by using finite difference method. Where appropriate, we use centered difference method for space derivatives. The singularity at $\mathrm{r} = 0$ is avoided by using the operator value $\frac{\partial^2}{\partial \mathrm{r}^2}$ as an approximation for $\frac{1}{\mathrm{r}}\frac{\partial}{\partial \mathrm{r}}$ for $\mathrm{r} = 0$ only. The motivation for this approximation is that both $\frac{\partial u}{\partial \mathrm{r}}$ and $\frac{\partial \phi}{\partial \mathrm{r}}$ are zero at $\mathrm{r} = 0$ [23].

An adequate number of mesh points on the domain are necessary for the accurate computation of ϕ in the interfacial region, which is costly since the mesh size has a strong influence on the speed and size of the computation. Let L be the number of the grids on each axis. We lay an LxL uniform mesh points over the domain such that 6 or 7 grids points are located at the interfacial region as measured from $\phi = -0.9$ to $\phi = 0.9$.

To solve the large sparse linear algebraic systems which arise from the discretization, we use a Fortran package ITPACK2C [24]. We perform the iteration twice for each time step $\triangle t = t_i - t_{i-1}$. First, we solve the equation which governs the phase field. We use this updated value and the initial values to solve the equation that governs the temperature. The iteration process for each time step is controlled by a loop to compute ϕ and u at the time $t_i = t_{i-1} + \triangle t$, $i = 1, 2, 3, ..., \mathrm{T}$.

Through out the computations, we set $L = 600$. Thus the uniform mesh size is $h = 1/L$ with a time step $\Delta t = 0.005$ and the free parameter is set at $\epsilon = h$. The true values of d_0, D and σ_0 for SCN are given by 2.83x10^{-7}cm, 1.147x10$^{-3} cm^2/s$ and 8.9 $ergs/cm^2$, respectively [25]. Under these conditions, the diffusion length, D/v_n, is at least 20 times larger than the tip, R_0, satisfying the standard theoretical conditions for dendritic growth [14]. Moreover, we set M = 4 and $\theta_0 = \pi/2$ so that the solid protrudes further in the vertical and the horizontal directions in accordance with 4-fold symmetry.

In order to address the issue raised in (A) and (B) above we consider nine dimensionless supercooling values from the microgravity experiments (IDGE) for SCN [20]. The computations for 20 seconds confirm that there is a linear relation between the supercoolings and corresponding growth velocites (Figure 1 and 2) for SCN. Table I shows that the computed results for velocity are close to the experimental values for each of the (dimensionless) supercooling values 0.00610, 0.0079, 0.01, 0.0126, 0.0161 and 0.0205 and outside of the experimental error range for the values 0.0265, 0.0338 and 0.0437. The results are consistent with other phase field studies that confirm this linear relation (see e.g. [14]).

Next, we consider the issue discussed in (C) above. We note that other numerical studies involving anisotropy have usually assumed dynamical anisotropy. Here we use only the anisotropy that can be quantified from experiments, namely, the anisotropy of the surface tension, which an equilibrium quantity. For the supercooling 0.01, we perform three computations for different δ_σ values of 0.005, 0.01 and 0.03 to determine the influence of anisotropy on the tip velocity [see equation (5)]. The corresponding growth velocities for each δ_σ are 0.000524, 0.000527 and 0.00054 (cm/s), respectively. As mentioned earlier,

the surface tension anisotropy for PVA is much larger than that of SCN. The experiments suggest that the tip velocity is similar for both materials. However, the possible in difference in the kinetic coefficients between the two material does not allow one to conclude that the magnitude of anisotropy does not influence the tip velocity. Our computational studies, on the other hand, indicate that an order of magnitude change in the anisotropy coefficient does not change the tip velocity significantly, confirming the conclusion of the experimenters [21]. Moreover the shape of the dendrite also does not appear to be affected very much. Only the tip of the dendrite becomes sharper for larger anisotropy, also confirming the experimental results.

The comparison of the growth velocities in 2-D and 3-D are examined for the supercoolings values of 0.01, 0.0161 and 0.0265. Since exactly the same initial and boundary conditions are used in both computations, the tip velocities for 2-D and 3-D can be compared. The velocities corresponding to these supercoolings in 2-D are 0.00033, 0.0005, and 0.00066 (cm/s), respectively, compared with the values of 0.00058, 0.00083 and 0.0012 (cm/s) respectively. There is a ratio of 1.76 $\pm$0.1 between the 3-D and 2-D calculations. A ratio of approximately 2 would be suggested by the factor (D-1) arising from the generalized Gibbs-Thomson relation above under the assumptions that the tip temperature and curvature are similar in the two geometries, and the two terms on the right hand side have similar roles.

Finally, we examine the role of the kinetic coefficient, discussed in (E) above, by varying α while other parameters are fixed. We use the undercooling $\Delta U = 0.01$ with the kinetic coefficients 1.5x10^6, 3.0x10^6 and 3.5x10^6. The corresponding velocities for each

α are 0.00016, 0.00066 and 0.00083 (cm/s). This indicates a strong dependence on this parameter which is a physically measurable quantity. Hence, setting this parameter to zero, which may be convenient from some perspectives (see e.g. [14], [15]) appears to change the tip velocity significantly. This may be the reason for the conclusion in [14], p. 4347, that "For PVA the agreement between theory and experiment remains very poor." In other words, the approximation $\alpha \approx 0$ is not valid for some materials. The material constants for PVA and SCN differ in the magnitude of the anisotropy and, perhaps, the kinetic coefficient, α. We have demonstrated that the magnitude of the anisotropy (when altered by almost an order of magnitude) does not have a strong influence on the tip velocity, while the kinetic coefficient (when altered by much less than an order of magnitude) has a dramatic influence. Thus, our calculations suggest that the kinetic coefficient is perhaps responsible for the lack of agreement between computations (or theory) versus experiment. At present there is little theoretical evaluation and experimental data for this parameter [26]. In all other experiments in this paper, we used a value of $3.5 \text{x} 10^6$ which is obtained from (3) in the kinetic Gibbs-Thomson relation. Further experimental data on this parameter would be very useful for developing our understanding of dendritic phenomena.

Acknowledgements: Supported by NSF Grant No. DMS-9703530. We are grateful for data provided by Dr. M.B. Koss.

References:

[1] G.P. Ivantsov, Dokl. Akad. Nauk USSR 58, 567 (1947)

[2] Y. Kim, N. Provatas, N. Goldenfeld and J. Dantzig, Phys. Rev. E 59, 1 (1999)

[3] E. Ben-Jacob, N. Goldenfeld, B. Kotliar, and J. Langer, Phys. Rev. Lett. 53, 2110

(1984)

[4] D.A. Kessler, J. Koplik, and H. Levine, Phys. Rev. A 30, 3161 (1984)

[5] D.A. Kessler, J. Koplik, and H. Levine, Adv. Phys. 37, 255 (1988)

[6] E. Brener and V.I. Melnikov, Adv. Phys. 40, 53 (1991)

[7] Y. Pomeau and M.B. Amar, *Solids far from Equilibrium,* ed. C. Godreche (Cambridge University Press, Cambridge, England, 1991), p.365

[8] G. Caginalp, *The limiting behavior of a free boundary in the phase field Model,* Carnegie-Mellon Research Report 82-5 (1982)

[9] G. Caginalp, *Lecture Notes in Physics 216*, 216-226 (Applications of Field Theory to Statistical Mechanics, ed. L. Garrido) Springer, Berlin (1984).

[10] G. Caginalp, Material Instabilities In Continium Problems and Related Mathematical Problems Heriot-Watt Symposium(1985-1986) ed J.Ball, Oxford Science Publications, Oxford, England, 35-52 (1988)

[11] G. Caginalp, Arch. Rational Mech. Anal. 92, 205 (1986)

[12] G. Caginalp and E.A. Socolovsky, Appl. Math. Letters 2, 117-120 (1989)

[13] T. Abel, E. Brener, and H.M. Krumbhaar, Phys. Rev E 55, 7789 (1997)

[14] A. Karma and W-J. Rappel, Phys. Rev. E 57, 4323 (1998).

[15] A. Karma, Y.H. Lee, and M. Plapp, Phys. Rev. E 61, 3996 (2000).

[16] N. Provatas, N. Goldenfeld, and J. Dantzig, J.C. LaCombe, A. Lupulescu, M.B. Koss, M.E. Glicksman, R. Almgren Phys. Rev. Lett. 82, 4496 (1999)

[17] J.A. Warner, R. Kobayashi, and W.C. Carter, J.Cryst. Growth 211, 18 (2000)

[18] N. Provatas, N. Goldenfeld and J. Dantzig, J. Comp. Phys 148, 265 (1999)

[19] S-L. Wang, R.F. Sekerka, A.A. Wheeler, B.F. Murray, S.R. Coriell, J. Brown and G.B. McFAdden, Physica D 69, 189 (1993); see also L.L. Regel, W.R. Wilcox, D. Popov, and F.C. Li, Acta Astronautica 48 (2-3), 101 (2001)

[20] M.E. Glicksman, M.B. Koss and E.A. Winsa, Phys. Rev. Lett. 73, 573 (1994)

[21] M.E. Glicksman and N.B. Singh, J. Cryst. Growth 98 , 277 (1989)

[22] G. Caginalp and X. Chen, In *On The Evolution Of Phase Boundaries,* eds. E. Gurtin and G. McFadden, Vol 1, 1 (Springer -Verlag, NewYork, 1992)

[23] G.D. Smith, *Numerical Solution of PDE*, Oxford Applied Mathematics and Computing Science Series (1985)

[24] D.R. Kincad, J.R. Respess, D.M. Young, R. Grimes, ITPACK 2.0 User Guide, CNA-150, University of Texas, Austin, 78712 August 1979

[25] M.E. Glicksman, R.J. Schaefer and J.D. Ayers, Met. Mat. Trans. A 7, 1747 (1976)

[26] R. Sekerka, J. Cryst. Growth 154, 377 (1995)

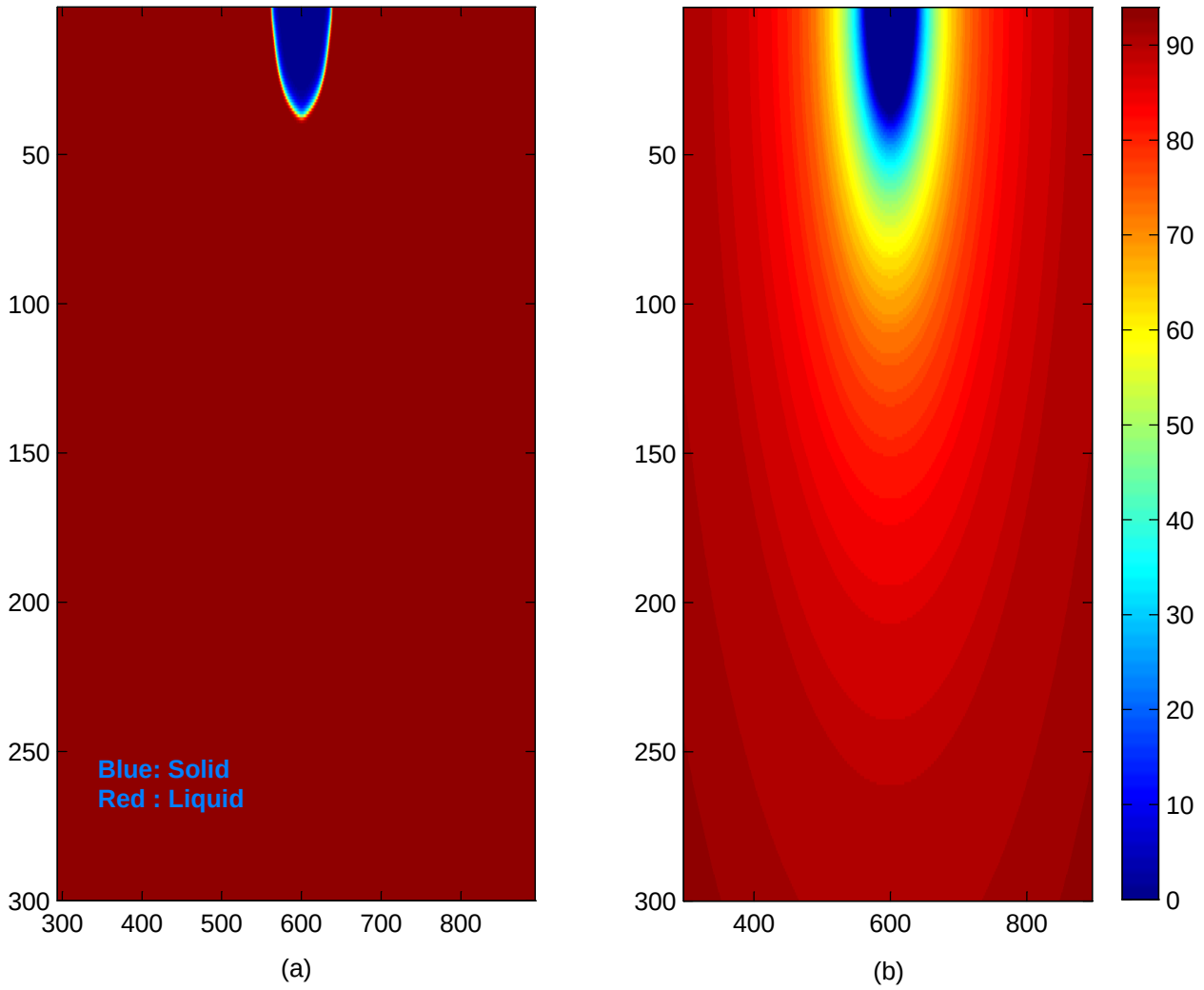

Fig1. The plots of the dendritic growth into melt for the supercooling 0.001. Fig 1(a) shows the phase field and Fig1 (b) shows the temperature field after 100seconds

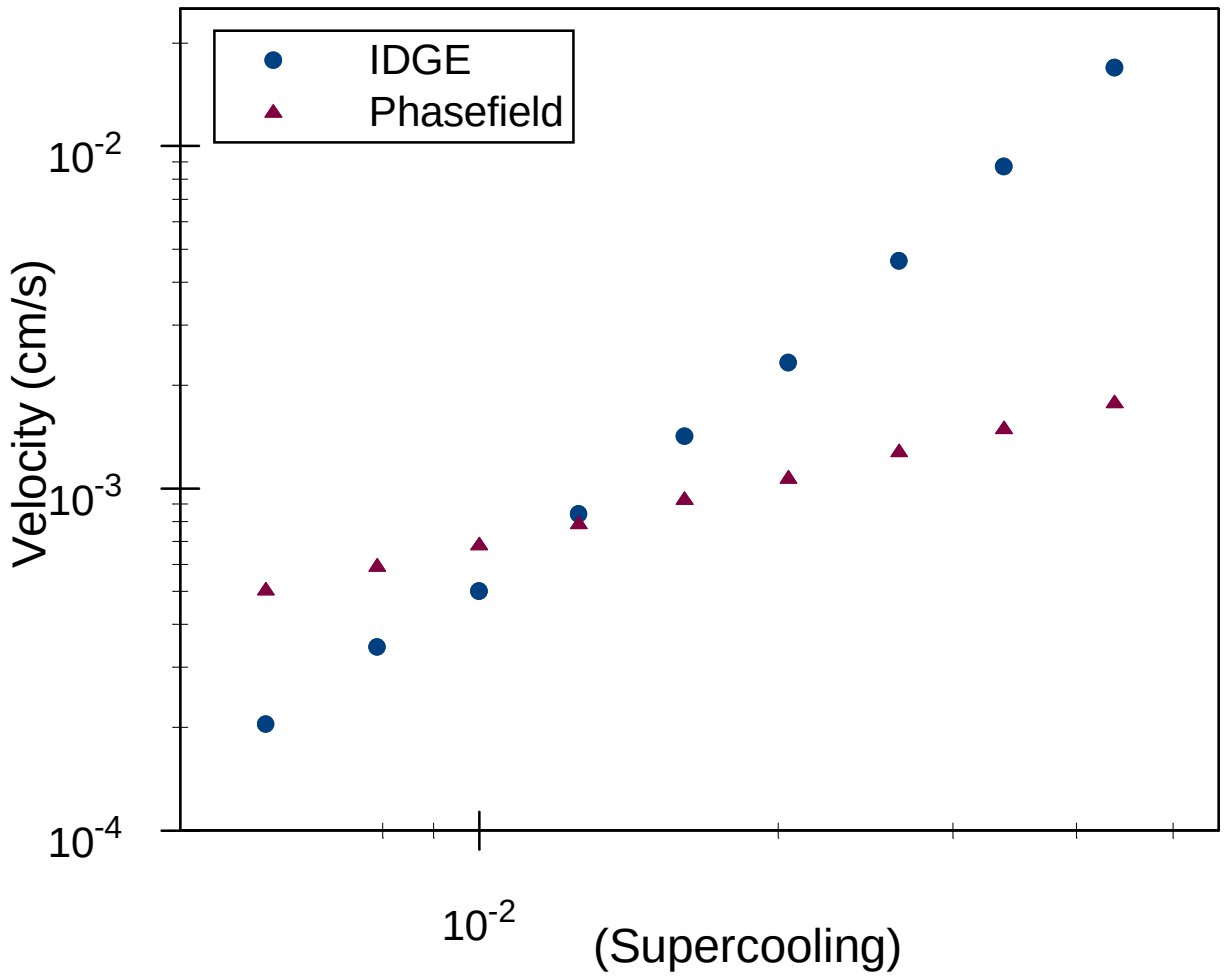

FIG.2. Dimensionless supercooling versus growth velocities (Log scales)

TABLE I. Microgravity dendritic growth velocity measurements calculated from telemetered binary images from the space shuttle Colombia (STS-62) and computational velocities

Supercooling	Velocity(IDGE) (cm/s)	Velocity(Computational) (cm/s)
0.04370	0.016980	0.001770
0.03380	0.008720	0.001486
0.02650	0.004620	0.001273
0.02050	0.002328	0.001066
0.01610	0.001417	0.000922
0.01260	0.000840	0.000784
0.01000	0.000500	0.000681
0.00790	0.000343	0.000590
0.00610	0.000204	0.000502